Catal Lett (2009) 130:19–27
DOI 10.1007/s10562-009-9884-3

Parallel Reactor Activity Studies of the Preferential Oxidation of CO on Transition Metals Supported on TiO_2 and TiO_2 Nanotubes

S. Guerrero · M. Di Serio · R. F. Li · E. E. Wolf

Received: 20 March 2008 / Accepted: 16 June 2008 / Published online: 24 February 2009

Abstract The preferential oxidation of carbon monoxide in the presence of hydrogen (PROX reaction) was studied on Cu catalysts promoted with Fe, Nb, Ce, and Ni supported on TiO_2 and on TiO_2 nanotubes. The surface area of the untreated TiO_2 anatase (150 m^2/g) support was increase to 350 m^2/g when transformed into TiO_2 nanotubes (NT). XRD and SEM results confirm the formation of nanotubular structures responsible of the increase in BET surface area. The activity results indicate that a 10% Cu/5% Nb/TiO_2-NT catalyst is highly active for this reaction compared to other transition metals and with a catalyst with the same composition supported on untreated TiO_2. We found close to 80% CO conversion and 40% selectivity to CO_2 formation at 170 °C. The higher activity is ascribed to a higher dispersion of Cu on the TiO_2 NT structures.

Keywords PROX · Transition metals · TiO_2 nanotubes

S. Guerrero · E. E. Wolf (✉)
Chemical Engineering Department, University of Notre Dame, Notre Dame, IN 46556, USA
e-mail: Wolf.1@nd.edu

S. Guerrero
CIMAT, Departamento de Ingeniería Química y Biotecnología, Universidad de Chile, Santiago, Chile

M. Di Serio
Department of Chemistry, University of Naples "Federico II", Naples, Italy

R. F. Li
College of Chemistry and Chemical Engineering, Taiyun University of Technology, Taiyun, China

1 Introduction

TiO_2 is among the most studied transition metal oxide as catalysts and catalyst support. The Ti oxide surfaces are simple to analyze since stoichiometric, and nearly perfect surfaces can be easily prepared ([1] and references therein). Recently, it has been reported that TiO_2 powders subjected to a certain hydrothermal followed by acid treatment can evolve into nanotubular structures. Kasuga et al. [2], reported a straight and simple method for preparing TiO_2 nanotubes. They loaded a sample of TiO_2 powder (anatase phase) in a Teflon vessel, and mixed it with a solution of 10 M NaOH. This mixture was hydrotreated at 110 °C for 20 h and followed by washing with a 0.1 N HCl solution. This procedure increased the surface area of the TiO_2 powder from 150 to 400 m^2/g. Transmission electron microscopy (TEM) results revealed needle-shaped tubular structures with an approximate inner diameter of 5 nm, outer diameter of 8 nm, and 100 nm in length. Similar structures were obtained using rutile phase TiO_2 as the starting material [10]. These authors reported that the initial crystalline raw material was first converted into an amorphous phase after the alkali hydrotreatment, and subsequently transformed into nanotubes by the HCl washing step used to remove the excess Na in the sample. When the particles were removed immediately after the hydrotreatment, without being washed by HCl, they had plate-shaped structures with low surface area. In contrast, the samples washed in HCl became needle-shaped with high surface area.

Sun and Li [3], using a similar procedure as described above, suggested the formation of a kind of titanate nanotube; $Na_xH_{2-x}Ti_3O_7$ ($x \approx 0.75$). They found that the presence of remaining ions in solution after hydrothermal treatment played an important role in the stability of the

nanotubes framework. After 3 days of washing, the suspension pH was reduced from 11 to 8. To adjust the pH to 7, diluted HCl was added and formation of some titanate sheets was observed. These authors concluded that as the sample is washed with dilute HCl, the sodium ions in the sample exchange with protons, which reduced the electronic interaction between the titanate sheets. They suggested that a molar ratio of Na to Ti of 1:4 is favorable to permit the formation of titanate nanotubes and preserve its morphology after calcination. Bavykin et al. [4], found that at a molar ratio of 0.00083 g TiO_2/mL NaOH, the resulting TiO_2 agglomerated into spherical particles of 1–2 mm size. At 0.03 g TiO_2/mL NaOH, the TiO_2 nanotubes agglomerate into random shaped particles of more than 4 μm diameter. This difference in shape was attributed to the slow convection inside the vessel during the hydrotreatment.

Studying the mechanism of TiO_2 nanotube formation, Tsai and Teng [5] found that the NaOH treatment induces the breaking of Ti–O–Ti bonds, forming an intermediate rich in Ti–O–Na and Ti–OH groups, which is facilitated by the H^+ exchange with Na^+ in the interlayer. The rearrangement of these intermediates evolves in the formation of sheets of edge-sharing TiO_6 octahedra with Na^+ and hydroxyl ions intercalated between sheets. In a similar way, Yao et al. [6], observed that the crystalline TiO_2 undergoes delamination during the treatment with NaOH, producing single layers of TiO_2. They observed that formation of TiO_2 NT from single sheets occurred in the [001] direction, followed by attraction of other sheets to surround the tubes. At temperatures higher than 90 °C, single layers of TiO_2 form with the (010) lattice planes parallel to the sheet surface. No formation of TiO_2 was observed when the same alkali treatment was done on amorphous TiO_2.

Zhang et al. [7] studied the thermal stability of the TiO_2 nanotubes and found a strong dependence of the surface area on the calcination temperature used. These authors proposed two types of dehydration of the material under calcination: (1) $H_2Ti_2O_4(OH)_2 \rightarrow H_2O + H_2Ti_2O_5$, and (2) $H_2Ti_2O_5 \rightarrow H_2O + 2TiO_2$(anatase). The first step corresponds to desorption of physically adsorbed water and intralayer water (H-bonded water in a layer), and the second dehydration involves desorption of interlayered water (water between layers). The second dehydration is accompanied by a phase transition from orthorhombic system to anatase and the collapse of the nanotubes. Increasing the temperature from room temperature to 300 °C decreased slightly the specific surface area S (S_{RT} = 402 m^2/g, $S_{300°C}$ = 354 m^2/g). Above 300 °C, the nanotubes broke and the surface area decreased sharply ($S_{400°C}$ = 190 m^2/g, $S_{500°C}$ = 118 m^2 g, $S_{600°C}$ = 50 m^2/g).

In this work, we used TiO_2 in various forms, but mainly as nanotubes, as support of transition metals catalysts for the preferential oxidation of CO (PROX). This reaction has been extensively studied on noble metal to remove CO from hydrogen prior to ammonia synthesis. In an early work at Engelhard [8], a 5% Pt supported on Al_2O_3 promoted with Fe, was impregnated in a monolith, giving 100% CO conversion and 51% selectivity at 90 °C. Later, Oh and Sinkevitch [9], used other noble metals (Pt, Pd, Rh and Ru) and found that the 0.5% Ru/Al_2O_3 and 0.5% Rh/Al_2O_3 catalysts were very selective. Gold-based catalysts are active for the PROX reaction at low temperatures [10]. In contrast to Pt catalysts, Au does not become saturated with CO, and oxygen adsorption is not inhibited by CO. Transition metals have also being studied for the PROX reaction. Copper catalyst were used as early as 1922, when Lamb et al. selectively oxidized CO in a H_2 rich stream using a mixture of copper and manganese [11]. Recently, CuO–CeO_2 catalysts [12–20] has shown total CO conversion between 100 and 150 °C, although selectivity decreased with temperature and time on stream [21]. The same authors compared three very active catalysts, 2.9% Au/FeO_2, 1.9% CuO–CeO_2, and 5% Pt/Al_2O_3, and found that at lower temperatures, Au was more active and selective but sensitive towards deactivation [22].

Finding less expensive and more active catalysts for the PROX reaction is a challenge in hydrogen purification for fuel cells. In this work we report the activity of different transition metals during the preferential oxidation of CO by using TiO_2 as support. In previous work we reported that when supported on TiO_2, Pt exhibited enhanced activity [23] for the PROX reaction. In this work we present results on the activity of transition metal catalysts supported on TiO_2. The novelty of this work reside in the use of the alkali method used by Kasuga et al. [2] to prepare TiO_2 nanotubes in addition to the use of commercial TiO_2 powders as support for transition metal catalysts.

2 Experimental

2.1 Catalysts Preparation

The TiO_2 powders used as support were obtained from Degussa. In addition, a multilayered silica-grafted TiO_2 (TSM) support with 240 m^2/g BET area was also used. This was prepared using SiO_2 (GRACE S-432) pre-calcined at 500 °C for 8 h as support. This calcined SiO_2 was contacted with a solution of titanium tetra-isopropoxide (Fluka) dissolved in dioxane, at room temperature. An amount of alkoxide corresponding to about 1.5 times the monolayer on silica was used. The maximum quantity of TiO_2 that can be grafted on silica in a single step (monolayer) was determined previously by an adsorption study of titanium isopropoxide dissolved in dioxane [24].

The resulting solids were filtered, washed with dioxane solvent, and dried overnight at 120 °C. Then, they were heated at 200 °C for 2 h and calcined at 500 °C for 2 h to eliminate any residual alkoxide groups. The amount of adsorbed titanium (7.5% TiO_2) determined by colorimetric analysis [25], was in agreement with previous data [24]. The grafting procedure was repeated three times in order to graft 17.4% TiO_2 onto the SiO_2 support.

Based on literature results, we selected the following transition metals for study: Cu, Ni, and Fe, single promoted with Nb oxide, and Ce oxide supported in various types of TiO_2 powders. As Cu was the most active catalyst, it was doubly promoted with Fe and Ni. The selected metals and oxides precursors were copper (II) nitrate hemipentahydrate (Aldrich), cerium (III) nitrate hexahydrate (Aldrich), ammonium niobate (V) oxalate hydrate (Aldrich), iron (III) nitrate nonhydrate (Aldrich). The proper amount of TiO_2 support was added to a Teflon container (1.625 in OD, 5 in long) and mixed with 50 mL of a solution containing 1% weight of the selected transition metal precursor (5% in the case of Nb). Then the Teflon container was sealed into an aluminum vessel and hydrotreated at 200 °C overnight. The resulting powder was filtered, washed with distilled water, and calcined at 300 °C for 2 h. When needed, successive impregnations of the other component were made on the M-TiO_2 catalyst (M: selected metal).

TiO_2 nanotubes were prepared following the procedure described by Kasuga et al. [2]. Two grams of TiO_2 (Aldrich, 99.7% anatase) are mixed with 60 mL of a solution of 10 M NaOH in a Teflon container (1.625 in OD, 5 in long) and hydrotreated at 110 °C for 24 h. The resulting suspension was washed with distilled water and then mixed with 50 mL of a 0.1 M HCl solution. This mixture was sonicated for 30 min and left overnight at room temperature. The resulting material was washed and dried at room temperature overnight. Wet impregnation of selected catalytic precursors on the TiO_2 nanotubes was carried out after drying the support at 110 °C for 2 h. After impregnation, the catalysts were calcined in air at 250 °C for 2 h.

2.2 Activity Measurements

The activity of the catalysts was measured in two types of reactors: a ten well parallel reactor, which permitted rapid evaluation of activity and selectivity, and a single tubular reactor for detailed activity measurements of selected samples. Both reactors used the same feed and temperature control systems. The reactants flow rates were kept constant by electronic mass flow controllers. A temperature controller, using a feedback from a thermocouple placed in a thermo-well located in the center of the catalyst bed, controlled an electrical heater and maintained the reactor temperature constant (±0.1 °C). The catalyst powders obtained from the preparations described above were first pelletized and the resulting pellets broken up to a powder that was sieved to yield agglomerates with average particle sizes of about 1 mm.

The parallel reactor consisted of 10 channels allowing the study of 10 samples at the same time. A quartz sleeve was inserted in each one of the channels containing 100 mg of each sample to allow rapid exchange of catalysts samples. As a reference, one of the channels was loaded with glass beads, and no reaction was observed in this channel. A mixture consisting of 1%CO, 2%O_2, 40% H_2, balance He, flowing at 600 cc/min was introduced in the main inlet of the 10-channel reactor (i.e. at about 60 cc/m per channel). The effluent from each channel was connected to a 10-port valve, which selected a single channel for GC analysis while bypassing the other channels. Analyses were done sequentially after reaching a steady temperature. Prior to reaction, the catalysts were reduced in 600 cc/min of a 1:1 H_2/He mixture at 200 °C for 1 h. After reduction, the reactor was cooled to room temperature and the reaction mixture was introduced. Then the reactor temperature was increased at a rate of 1 °C per min. The 10 port parallel reactor permitted rapid evaluation of the activity and selectivity of several catalysts preparations. The most interesting catalysts were then studied in detail in a single tubular reactor described below.

The flow tubular quartz reactor has a 1 cm ID and 30 cm long, and it was loaded with 200 mg of catalyst. This reactor is equipped with an external diaphragm pump (Thomas Industries) to provide an external recycle loop use during kinetic studies. The recycle ratio (total flow rate/feed flow rate) was about 20 to ensure conditions of perfect mixing and to eliminate diffusional mass and heat-transport effects during reaction. The perfect mixing conditions permitted the direct calculation of reaction rates in a much broader range of reaction conditions (up to 100% conversion) that it can be attained under differential reaction conditions normally used in single pass plug flow reactors (i.e. less than 10% differential conversion). Prior to each run, the catalysts were reduced in situ in a stream of pure hydrogen flowing at 50 cc/min for 1 h at 200 °C. The same activity results were obtained at higher reduction temperatures. After cooling the reactor to room temperature and purging with helium, the reaction mixture with a composition of 0.8% CO, 0.8% O_2, and 51% H_2, with He as balance, was added at a total flow rate of 195 cc/min. Experiments were conducted by increasing linearly the reactor temperature at 1 °C/min until reaching 200 °C.

Samples from the gaseous effluent were analyzed on line using a gas chromatograph (Varian 3700) equipped with a CTR I (Alltech) and a molecular sieve (Alltech) columns, mounted in parallel, and maintained at 50 °C using He as a

carrier at 120 cc/min. This column arrangement allows separating H_2, CO, O_2, CO_2, and CH_4. The latter gas was not detected in any experiment. Selectivity is defined as the ratio between oxygen consumed in the selective oxidation of CO versus the total amount of oxygen consumed and it was calculated as: $S_e = P^{out}_{CO_2}/2\left(P^{in}_{O_2} - P^{out}_{O_2}\right)$.

2.3 X-ray Diffraction (XRD)

The X-ray diffractometer utilized in this work was a Scintag X-1 using Cu Kα radiation at a wavelength of 0.1540562 nm. Approximately 100 mg of a finely crushed and sieved sample were homogenously dispersed onto a silica or glass holder. The diffracted X-rays from the sample were detected by a Peltier cooled solid-state detector moving in a circular pattern. The 2θ angle was scanned from 20° to 90° with a step size of .05°. Depending on the analysis, the scan rate was constant at 0.1 degrees per second or 0.5 s per step.

2.4 Scanning Electron Microscopy (SEM)

Scanning electron microscopy imaging was done in a Hitachi S4500 field emission SEM operating at 30 keV under a vacuum of 10^{-6} torr. Prior to SEM analysis the samples were finely grounded and mounted in a carbon tape on the specimen holder. Alternatively, to improve the particle dispersion on the holder, 2 mg of the grounded sample was diluted in distilled water. Then, a drop of this suspension was set on the clean holder surface and evaporated at room temperature.

2.5 BET Measurements

The BET area of the catalysts was measured on a Quantachrome Monosorb unit operating at a nitrogen partial pressure of 0.3 in He. Approximately 50 mg of sample were outgassed at 200 °C for 1 h prior to each measurement, which were repeated several times to ensure reproducibility.

3 Results and Discussion

3.1 Activity Results

3.1.1 Mixed Oxides

Figure 1 shows the PROX results obtained in the parallel reactor for the 1% Cu–1% Fe/TiO_2, 1% Cu–5% Nb/TiO_2, 1% Cu/5% Nb/5% Ce/TSM, 1% Cu/TiO_2, 1% Cu–1% Ce/TiO_2, 1% Ni–/TiO_2, 1% Cu–1% Ni/TiO_2, and 1% Cu–5% Nb–1% Ce/TiO_2 catalysts. The activity of the 1% Ce/TiO_2, 1% Nb/TiO_2, and 1%Fe/TiO_2 catalysts was negligible and are not included in Fig. 1. The plain TiO_2 support, included as a reference, exhibits 17% CO and 21% O_2 conversion corresponding to 20% selectivity (Fig. 1). Given the CO conversion on the TiO_2 support, the required oxygen conversion to obtain 100% selectivity would be 4.3%. Thus the measured 20% selectivity on TiO_2 means that hydrogen is being oxidized to water on the TiO_2 support. Addition of 1% Cu to the TiO_2 support resulted in a catalyst with 16% CO and 11% O_2 conversions. Although the CO conversion on the 1% Cu/TiO_2 catalyst was similar to that obtained on the TiO_2 support, the lower O_2 conversion indicated that the CO_2 selectivity almost doubled with addition of Cu. When Fe or Nb was impregnated with Cu and supported on TiO_2, all the activities increased significantly. As shown in Fig. 1a, the 1% Cu–1% Fe/TiO_2 and 1% Cu–5% Nb/TiO_2 catalysts were the most active showing 53 and 60% CO conversion at 200 °C, respectively. The 1% Cu–5% Nb/TiO_2 catalyst showed higher CO and O_2 conversion at all temperatures. Interestingly the TSM support, which has higher TiO_2 area, did not exhibit higher conversion than the regular TiO_2. The lower O_2 conversion obtained on the 1% Cu–1% Fe/TiO_2 catalyst led to a slightly higher selectivity than that obtained with the 1% Cu–5% Nb/TiO_2 catalyst. The rest of the catalysts exhibit CO conversions lower than 20%.

Figure 1c shows that at low temperature ($T < 100$ °C) the selectivity to CO_2 is high for all the catalysts which indicates that CO oxidation is mainly occurring below 100 °C. As the temperature increases, the selectivity to CO_2 gradually decreases in all catalysts. Infrared results discussed later, show that under reaction conditions the surface is saturated with CO at low temperature. The high coverage of CO inhibits hydrogen adsorption and reaction, resulting in high selectivity at low temperatures. As the temperature increases and CO gradually desorbs, hydrogen adsorbs on the empty sites and reacts to form water decreasing CO_2 selectivity. Since the simultaneous presence of Cu and Nb supported on TiO_2 resulted in a highly active catalyst for preferential CO oxidation under PROX conditions, the Cu–Nb/TiO_2 catalyst was selected for further catalytic studies and characterization.

The effect of copper loading in the PROX reaction was also studied in the parallel reactor using a fixed 5%Nb loading (Fig. 2).

No direct correlation between CO conversion and copper loading is apparent in Fig. 2a. However, the 10% Cu/5% Nb/TiO_2 catalyst shows a maximum of 94% CO conversion at 160 °C, that decreases at higher temperatures. The rest of the catalysts show increasing CO conversion with temperature, with a maximum of 90% at 200 °C for the 0.5% Cu/5% Nb/TiO_2 catalyst. All the catalysts show an increasing O_2 conversion with

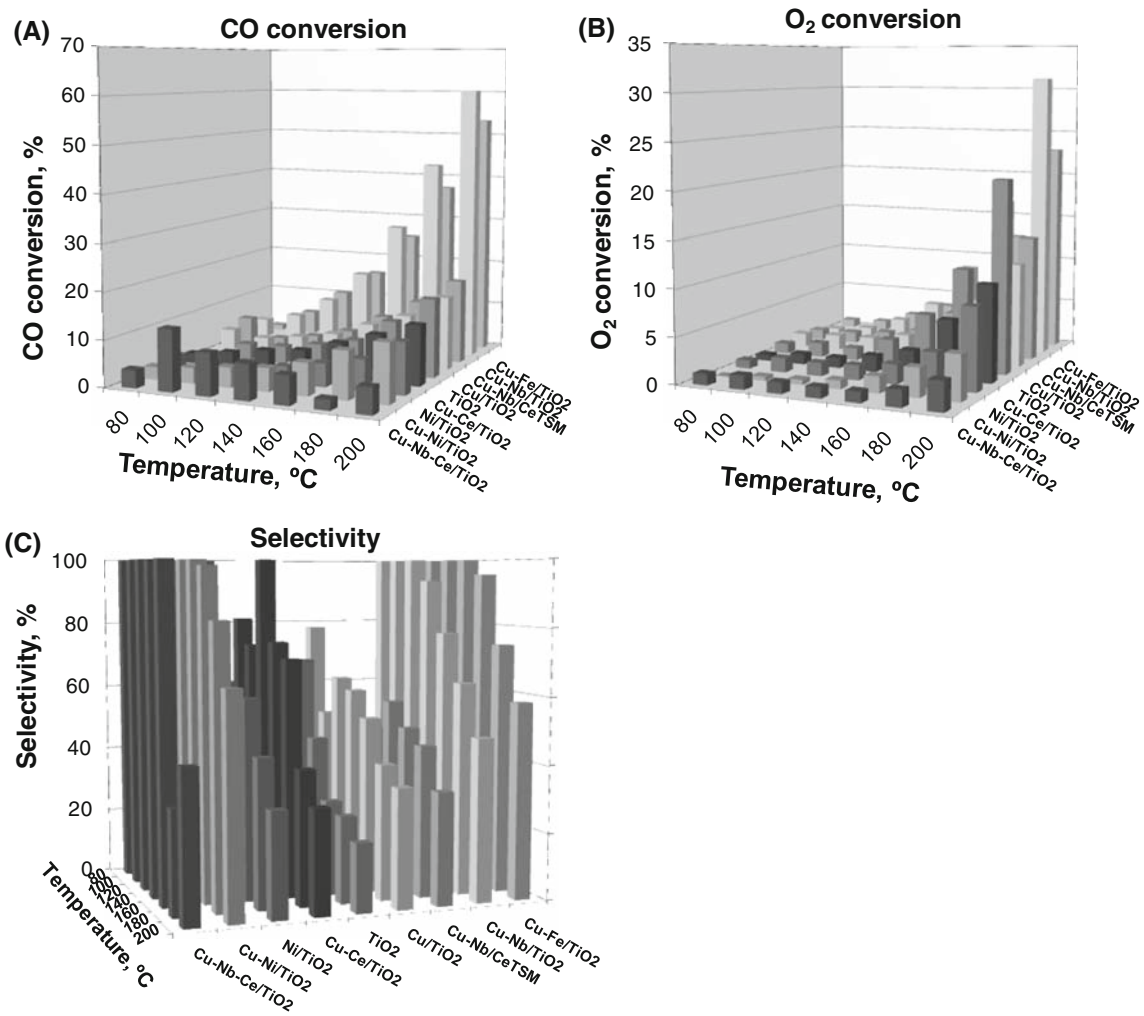

Fig. 1 PROX results in the parallel reactor. **a** CO conversion, **b** O_2 conversion, and **c** selectivity. Total flow: 600 cc/min. Catalysts mass: 100 mg. Concentrations: 1% CO, 2% O_2 40% H_2, balance He. Catalysts prereduced at 200 °C for 1 h

temperature, with the 10% Cu/5% Nb/TiO_2 catalyst being the most active with 99% O_2 conversion at 180–200 °C. The 0.5% Cu/5% Nb/TiO_2, 1% Cu/5% Nb/TiO_2, and 5% Cu/5% Nb/TiO_2, show 68, 20, and 60% O_2 conversion at 200 °C, respectively. The 10% Cu/5% Nb/TiO_2 catalyst shows near 70% CO selectivity at low temperature, but decreases to 29% at 160 °C. The CO selectivity of the 0.5% Cu/5% Nb/TiO_2, 1% Cu/5% Nb/TiO_2, and 5% Cu/5% Nb/TiO_2 catalysts show a maximum of 76, 74, and 66% at 140 °C, respectively.

Scanning electron microscopy micrographs of TiO_2-NT are shown in Fig. 3. Figure 3a shows a representative image of TiO_2 samples after drying and calcination at 250 °C. The micrograph, at a 100 K magnification, shows that the sample is made of a network of filaments or rods, which is responsible for the increase in surface area determined by BET. Work is underway by HRTEM to determine if these are nanotubes or nanorods but plenty of evidence in the literature indicates formation of nanotubes [2, 4, 26].

When the TiO_2-NT sample was calcined at 600 °C (Fig. 3b), the diameter of the rods grew and the void space between the rods decreased in agreement with the lower surface area of 50 m^2/g obtained by BET on calcined TiO_2-NT. Figure 3c shows a representative micrograph at 130 K magnification of a sample impregnated with Cu calcined at 250 °C.The micrograph shows similar characteristics as the TiO_2-NT support, indicating that Cu is highly dispersed in this sample with no evidence of the formation of a separate phase. The Cu containing sample calcined at 600 °C also shows the same coarse structure as Fig. 3b.

3.1.2 Cu–Nb Oxides Supported n TiO_2 Nanotubes

The most active catalyst composition 10% Cu/5% Nb, was selected for further studies on TiO_2 nanotubes as supports

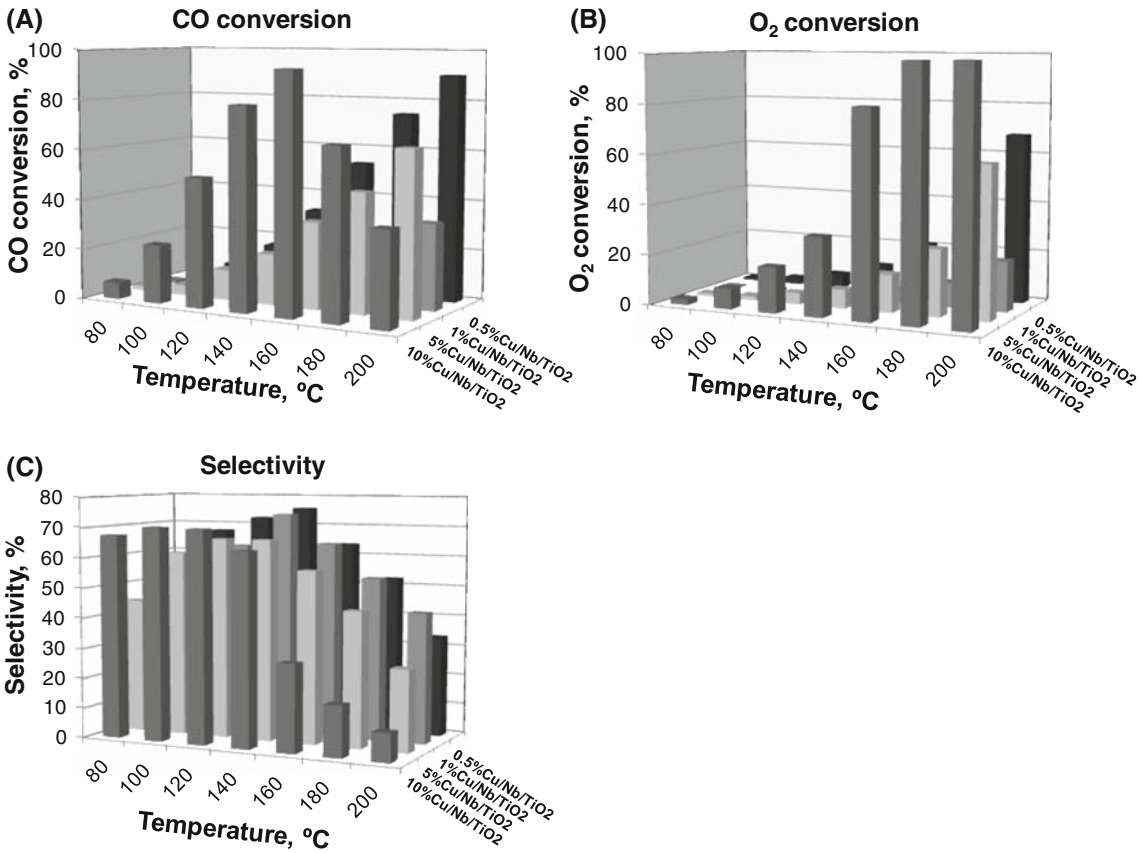

Fig. 2 PROX results in the parallel reactor for the X%Cu/5%Nb/TiO_2 catalysts ($X = 0.5$, 1, 5, and 10%). **a** CO conversion, **b** O_2 conversion, and **c** selectivity. Total flow: 600 cc/min. Catalysts mass: 100 mg. Concentrations: 1% CO, 2%O_2 40% H_2, balance He. Catalysts prereduced at 200°C for 1 h

(TiO_2-NT). The effect of the BET surface area on the PROX activity was studied in the parallel reactor with the 10% Cu/TiO_2 (50 m^2/g, Degussa), 10% Cu/5% Nb/TiO_2 (150 m^2/g, Aldrich) and 10% Cu/5% Nb/TiO_2-NT (350 m^2/g TiO_2 nanotubes) catalysts. The BET area was measured after impregnation with the precursor oxides.

Figure 4a compares the PROX activity of the 10%Cu/TiO_2 (50 m^2/g, Degussa), 10% Cu/5% Nb/TiO_2 (150 m^2/g, Aldrich) and 10% Cu/5% Nb/TiO_2-NT (350 m^2/g TiO_2 nanotubes) in terms of CO conversion versus temperature obtained in the parallel reactor. It can be observed that the CO conversion is slightly higher on the catalysts having higher surface area but certainly not proportional to the BET area. The 10% Cu/TiO_2 (50 m^2/g) is included for comparison and it shows lower CO conversion than the Nb-promoted catalysts.

To confirm the promotion effect of Nb on the PROX activity, the CO conversion on 10% Cu/5% Nb/TiO_2-NT and 10% Cu/TiO_2-NT catalysts, both with a BET surface area of 350 m^2/g, were compared. Fig. 4b shows the results on these catalysts obtained in the recycle reactor using half the contact time used in the parallel reactor. It can be observed that both the 10% Cu/5% Nb/TiO_2-NT and 10% Cu/TiO_2-NT catalysts have similar CO conversion. In fact, the Nb-promoted catalyst shows only a slightly higher CO conversion at high temperature. In contrast, the 10% Cu/5% Nb/TiO_2 (150 m^2/g, no nanotubes) catalyst shows lower activity but a similar CO conversion up to 150 °C, and then decreasing abruptly at higher temperatures.

As described in the experimental section, the preparation steps of the TiO_2 nanotubes include the use of a dilute HCl acid solution, which has been found to be essential in the formation mechanism of TiO_2 nanotubes [2, 3, 26]. After preparation of the TiO_2 nanotubes traces of chlorine can still remain in the support. To test the effect of chlorine, a new batch of TiO_2-NT was prepared. Part of the TiO_2 suspension after the alkali treatment was set apart and mixed with a solution of 0.1 M HNO_3 and left overnight. The rest of the suspension was mixed as usual with a solution of 0.1 M HCl and left soaking overnight. The latter suspension was divided into two parts. One part was left unwashed while the other was washed thoroughly with distilled water to reduce the content of chlorine from the TiO_2-NT support. Then these three supports were used to prepare a 10% Cu/5% Nb/TiO_2-NT catalyst by successive impregnation. The effect of chlorine on the PROX activity

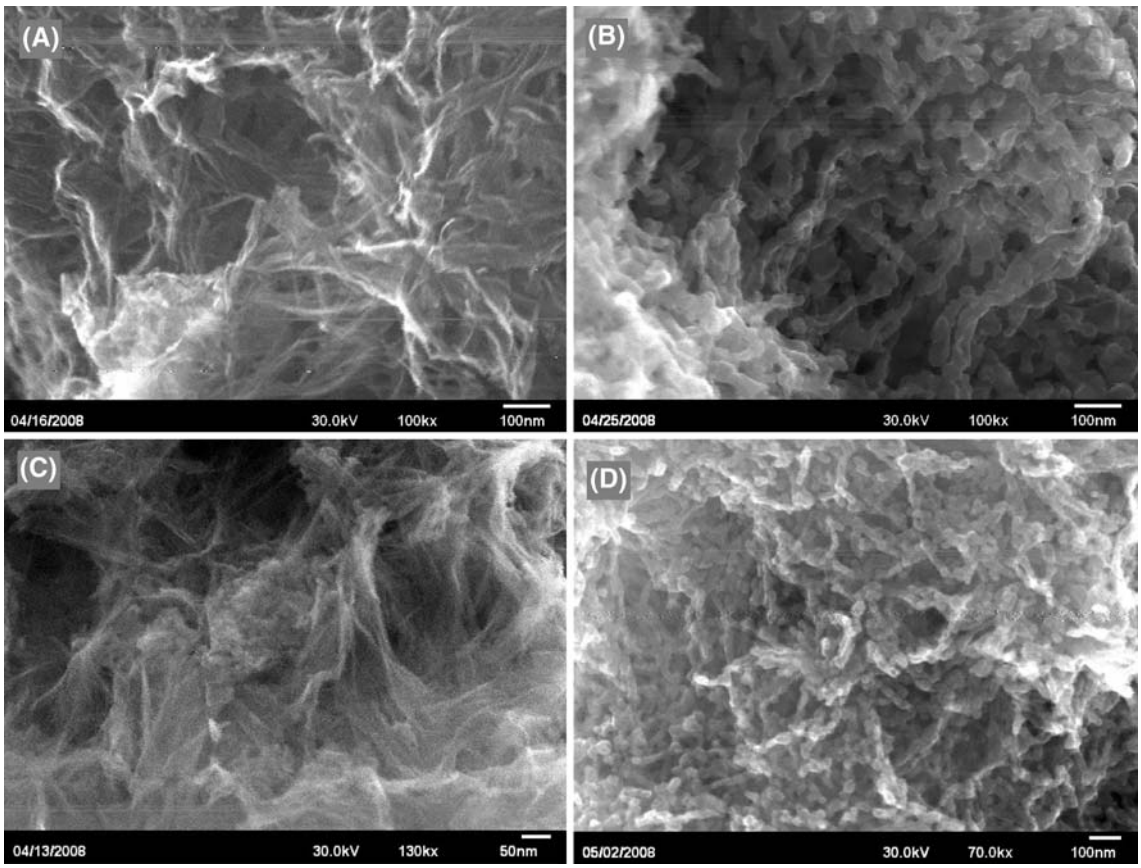

Fig. 3 SEM micrographs of **a** TiO_2-NT calcined at 250 °C, **b** calcined at 600 °C, **c** 10%Cu/TiO_2-NT calcined at 250 °C, and **d** 10%Cu/TiO_2-NT calcined at 600 °C

using these catalysts is shown in Fig. 4c. The chlorine-free catalyst shows a slightly better activity with a maximum of 81% CO conversion at 160 °C. The low-chlorine catalyst is more active than the one containing chlorine at low temperature, although both reach similar maximum CO conversions at high temperatures (169–177 °C). These results show that the presence of chlorine has some effect on the activity of the catalysts but is not too significant.

Figure 4d shows the selectivity to CO using a different batch of Cu/Nb/TiO_2 and Cu/TiO_2 catalysts. The scattered data indicates a similar trend, where the catalysts are more selective at low temperature and then their selectivities almost linearly decrease as the temperature increases. The average selectivity at the maximum CO conversion was 40%.

3.2 XRD Results

X-ray diffraction results of the 10% Cu/TiO_2-NT and 10% Cu/5% Nb/TiO_2-NT catalysts was carried out in air at room temperature. Before analysis, the samples were calcined in air at 250 °C for 2 h. The resulting patterns are presented in Fig. 5, along with those of the TiO_2-NT support and the untreated TiO_2 (anatase) powder used in the preparation of TiO_2-NT. The TiO_2 (anatase) diffraction lines from the International Centre for Diffraction Data (ICDD) is included at the bottom of Fig. 5.

The diffraction pattern of the TiO_2 powder clearly corresponds to TiO_2 anatase crystal phase. The diffraction pattern of the TiO_2-NT shows less intense lines with the main diffraction observed at $2\theta = 49^\circ$ and a less intense line at $2\theta = 25^\circ$ showing a left-shift which has been previously attributed to the presence of nanotubes structures [27]. No lines corresponding to Nb and Cu are observed on the copper containing catalysts. This observation indicates the presence of highly dispersed small copper and niobia particles in both samples.

The significant increase in the surface area of the TiO_2-NT support and their characteristic XRD diffraction patterns are an indication of the formation of TiO_2 nanotubes.

It remains to determine why the Cu–Nb catalysts supported on TiO_2 nanotubes structures exhibit higher activity than on untreated TiO_2. Clearly while the BET areas of the different supports vary significantly, this does not translate into higher activity. The XRD and SEM results suggest that the nanotubes help to disperse Cu on the TiO_2 surface.

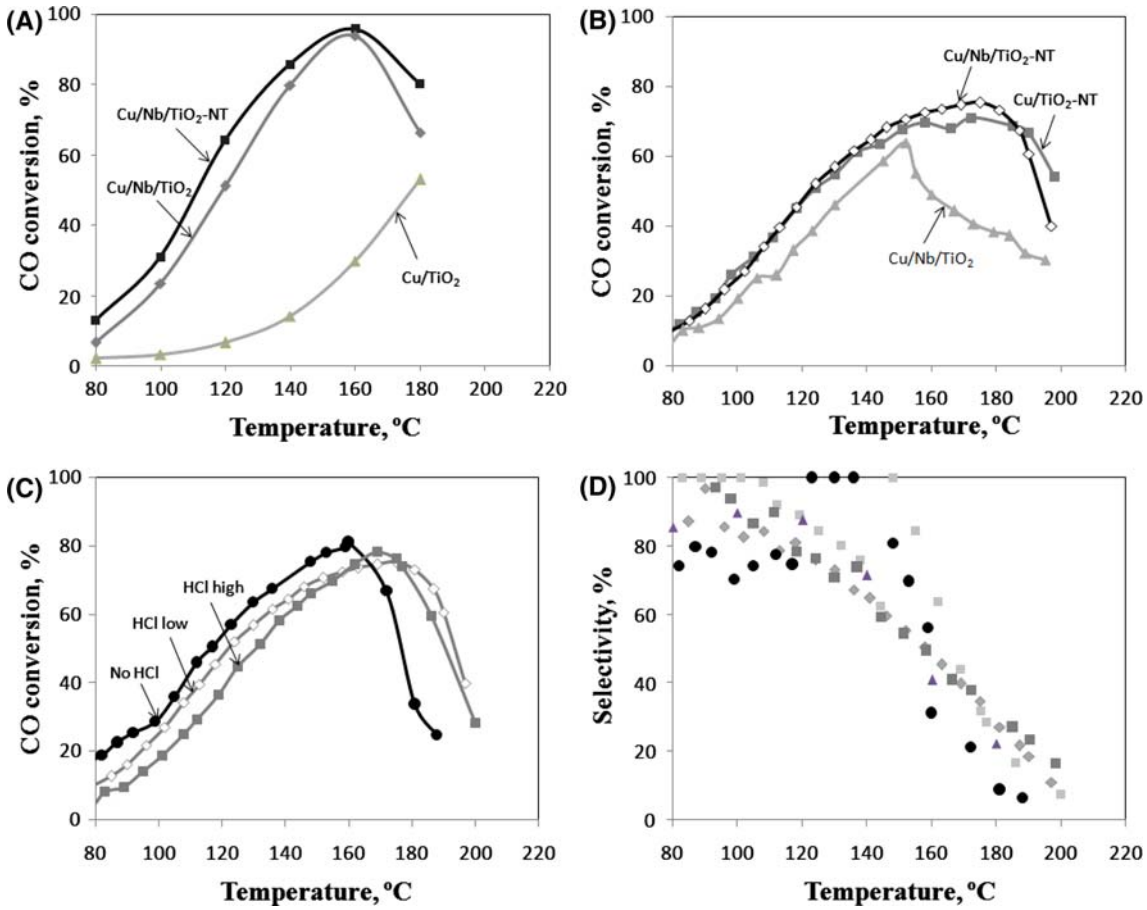

Fig. 4 PROX results in **a** the parallel reactor and **b** recycle reactor for the 10% Cu/5% Nb/TiO_2-NT, 10% Cu/5% Nb/TiO_2, and 10% Cu/TiO_2 catalytsts. The effect of HCl in the PROX activity is compared in **c** for the 10% Cu/5 %Nb/TiO_2-NT catalysts. **d** CO selectivity on the PROX reaction for Cu/Nb/TiO_2 catalyst prepared by different methods

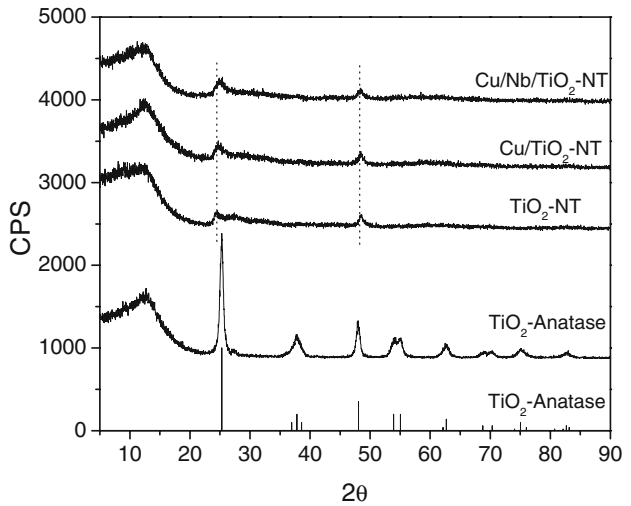

Fig. 5 XRD spectra from the 10% Cu/TiO_2-NT and 10% Cu/5% Nb/TiO_2-NT catalysts along with the TiO_2-NT support. The experimental spectrum measured from the raw TiO_2-anatase is included as reference along with its line spectrum from the ICDD database on the *bottom*

From previous work on Pt–Nb promoted catalysts it was found that the Nb phase altered the oxidation state of the Pt surface, an effect that depended critically on the Nb loading [27]. It is not unreasonable to assume that the Nb support could play a role in changing the oxidation state of the Cu surface, but such hypothesis needs to be proven and work is underway to do so. It should be pointed out that these catalysts are among the most active non-precious metals catalysts reported for the PROX reaction.

4 Conclusions

The activity of Cu supported on TiO_2 was investigated, along with the promotional effect of adding Fe, Nb, Ce, and Ni. The results show that Cu supported on TiO_2 is active in the PROX reaction, and that the reaction is promoted by addition of Nb. It was also found that the activity was improved when the support consisted of TiO_2 nanotubes. In fact, a 10%Cu/5%Nb/TiO_2-NT catalyst showed

close to 80% CO conversion at around 170 °C. It is speculated that the use of nanotubes increased Cu dispersion and thus its activity. The use of TiO_2 nanotubular structures as support constitutes an interesting alternative to increase dispersion or change in oxidation state that can affect the activity and selectivity of a catalyst.

Acknowledgments The support of this work by a Bayer Postdoctoral Fellowship in Environmental Chemistry through the Center for Environmental Science and Technology at the University of Notre Dame is gratefully acknowledged.

References

1. Henrich EV, Cox PA (1994) The surface science of metal oxides. Cambridge University Press, Cambridge
2. Kasuga T, Hiramatsu M, Hoson A, Sekino T, Niihara K (1998) Formation of titanium oxide nanotube. Langmuir 14(12):3160–3163
3. Sun X, Li Y (2003) Synthesis and characterization of ion-exchangeable titanate nanotubes. Chem Eur J 9:2229–2238
4. Bavykin DV, Parmon VN, Lapkin AA, Walsh FC (2004) The effect of hydrothermal conditions on the mesoporous structure of TiO_2 nanotubes. J Mater Chem 14:3370–3377
5. Tsai C-C, Teng H (2006) Structural features of nanotubes synthesized from NaOH treatment on TiO_2 with different post-treatments. Chem Mater 18:367–373
6. Yao BD, Chan YF, Zhang XY, Zhang WF, Yang ZY, Wang N (2003) Formation mechanism of TiO_2 nanotubes. Appl Phys Lett 82(2):281–283
7. Zhang M, Jin Z, Zhang J, Guo X, Yang J, Li W, Wang X, Zhang Z (2004) Effect of annealing temperature on morphology, structure and photocatalytic behavior of nanotubed $H_2Ti_2O_4(OH)_2$. J Mol Catal 217:203–210
8. Korotkikh O, Farrauto R (2000) Selective catalytic oxidation of CO in H_2 fuel cell applications. Catal Today 62:249–254
9. Oh SH, Sinkevitch RM (1993) Carbon monoxide removal from hydrogen-rich fuel cell feedstreams by selective catalytic oxidation. J Catal 142:254–262
10. Torres Sanchez RM, Ueda A, Tanaka K, Haruta M (1997) Selective oxidation of CO in hydrogen over gold supported on manganese oxides. J Catal 168(1):125–127
11. Lamb AB, Scalione CC, Edgar G (1922) The preferential catalytic combustion of carbon monoxide in hydrogen. J Am Chem Soc 44:738–756
12. D. Gamarra, A. Hornes, Z. Koppany, Z. Schay, G. Munuera, J. Soria, A. Martinez-Arias (2007) Catalytic processes during preferential oxidation of CO in H_2-rich streams over catalysts based on copper-ceria. J Power Sour CONAPPICE—Selected papers presented at the 2nd National Congress on fuel cells (CONAPPICE 2006), Madrid, Spain, 18–20 October 2006. 169(1):110–116
13. Gamarra D, Munuera G, Hungria AB, Fernandez-Garcia M, Conesa JC, Midgley PA, Wang XQ, Hanson JC, Rodriguez JA, Martinez-Arias A (2007) Structure-activity relationship in nanostructured copper–ceria based preferential CO oxidation catalysts. J Phys Chem C 111(29):11026–11038
14. Sedmak G, Hocevar S, Levec J (2003) Kinetics of selective CO oxidation in excess of H_2 over the nanostructured $Cu_{0.1}Ce_{0.9}O_{2-y}$ catalysts. J Catal 213:135–150
15. Liu Y, Fu Q, Stephanopoulos MF (2004) Preferential oxidation of CO in H_2 over CuO–CeO_2 catalysts. Catal Today 93–95:241–246
16. Park JW, Jeong JH, Yoon WL, Rhee YW (2004) Selective oxidation of carbon monoxide in hydrogen-rich stream over Cu–Ce/g–Al_2O_3 catalysts promoted with cobalt in a fuel processor for proton exchange membrane fuel cells. J Power Sour 132:18–28
17. Ratnasamy P, Srinivas D, Satyanarayana CVV, Manikandan P, Senthil Kumaran RS, Sachin M, Shetti VN (2004) Influence of the support on the preferential oxidation of CO in hydrogen-rich steam reformates over the CuO–CeO_2–ZrO_2 system. J Catal 221(2):455–465
18. Manzoli M, Monte RD, Boccuzzi F, Coluccia S, Kaspar J (2005) CO oxidation over CuO_x–CeO_2–ZrO_2 catalysts: transient behaviour and role of copper clusters in contact with ceria. Appl Catal B 61(3–4):192–205
19. Mariño F, Descorme C, Duprez D (2005) Supported base metal catalysts for the preferential oxidation of carbon monoxide in the presence of excess hydrogen (PROX). Appl Catal B 58(3–4):175–183
20. Martinez-Arias A, Hungria AB, Fernandez-Garcia M, Conesa JC, Munuera G (2005) Preferential oxidation of CO in a H_2-rich stream over CuO/CeO_2 and CuO/(Ce, M)Ox (M = Zr, Tb) catalysts. J Power Sour 151:32–42
21. Avgouropoulos G, Ioannides T, Matralis HK, Batista J, Hocevar S (2001) CuO–CeO_2 mixed oxide catalysts for the selective oxidation of carbon monoxide in excess hydrogen. Catal Lett 73:33–39
22. Avgouropoulos G, Ioannides T, Papadopoulou C, Batista J, Hocevar S, Matralis HK (2002) A comparative study of Pt/g–Al_2O_3, Au/a–Fe_2O_3 and CuO–CeO_2 catalysts for the selective oxidation of carbon monoxide in excess hydrogen. Catal Today 75:157–167
23. Li W, Gracia FJ, Wolf EE (2003) Selective combinatorial catalysis; challenges and opportunities: the preferential oxidation of carbon monoxide. Catal Today 81:437–447
24. Santacesaria E, Cozzolino M, Di Serio M, Venezia AM, Tesser R (2004) Vanadium based catalysts prepared by grafting: preparation, properties and performances in the ODH of butane. Appl Catal 270:177–192
25. Snell FRD, Ettre LS (1974) Encyclopedia of industrial chemical analysis, vol 19. Interscience, New York, p 107
26. Kasuga T, Hiramatsu M, Hoson A, Sekino T, Niihara K (1999) Titania nanotubes prepared by chemical processing. Adv Mater 11(15):1307–1311
27. Zhu B, Zhang X, Wang S, Zhang S, Wu S, Huang W (2007) Synthesis and catalytic performance of TiO_2 nanotubes-supported copper oxide for low-temperature CO oxidation. Microporous Mesoporous Mater 102:333–336